Microbial food webs and metabolic state across oligotrophic waters of the Mediterranean Sea during summer

Urania Christaki, France van Wambeke, Dominique Lefèvre, A. Lagaria, L. Prieur, Mireille Pujo-Pay, J. -D. Grattepanche, J. Colombet, S. Psarra, J. R. Dolan, et al.

Biogeosciences, 8, 1839–1852, 2011
www.biogeosciences.net/8/1839/2011/
doi:10.5194/bg-8-1839-2011

Biogeosciences

Microbial food webs and metabolic state across oligotrophic waters of the Mediterranean Sea during summer

U. Christaki[1], F. Van Wambeke[2], D. Lefevre[2], A. Lagaria[1,3], L. Prieur[4,8], M. Pujo-Pay[5,6], J.-D. Grattepanche[1], J. Colombet[7], S. Psarra[3], J. R. Dolan[4,8], T. Sime-Ngando[7], P. Conan[5,6], M. G. Weinbauer[4,8], and T. Moutin[9]

[1]INSU-CNRS, UMR8187 LOG, Laboratoire d'Océanologie et des Géosciences, Université Lille Nord de France, ULCO, 32 avenue Foch, 62930 Wimereux, France
[2]INSU-CNRS, UMR6117, LMGEM, Laboratoire de Microbiologie, Géochimie et Ecologie Marines, Université de la Méditerranée, Centre d'Océanologie de Marseille, Campus de Luminy Case 901, 13 288 Marseille cedex 9, France
[3]Hellenic Centre for Marine Research, Institute of Oceanography, 71003 Heraklion, Crete, Greece
[4]INSU-CNRS, UMR7093 LOV, Laboratoire d'Océanographie de Villefranche, Observatoire Océanologique de Villefranche-sur-Mer, 06 238 Villefranche-sur-Mer, France
[5]INSU-CNRS, UMR7621, Lab. d'Océanographie Microbienne, Observatoire Océanologique, 66651 Banyuls/mer, France
[6]UPMC Univ Paris 06, UMR7621, Laboratoire d'Océanographie Microbienne, Observatoire Océanologique, 66651 Banyuls/mer, France
[7]INSU-CNRS, UMR6023, LMGE, Laboratoire Microorganismes: Génome et Environnement – 63177 Aubière cedex, France
[8]UPMC Univ Paris 06, UMR7093, Laboratoire d'Océanographie de Villefranche, Observatoire Océanologique de Villefranche-sur-Mer, 06230 Villefranche-sur-Mer, France
[9]INSU-CNRS, UMR6535, LOPB, Laboratoire d'Océanographie physique et biogéochimique Université de la Méditerranée, Centre d'Océanologie de Marseille, Campus de Luminy Case 901, 13 288 Marseille cedex 9, France

Received: 6 December 2010 – Published in Biogeosciences Discuss.: 10 January 2011
Revised: 8 June 2011 – Accepted: 10 June 2011 – Published: 12 July 2011

Abstract. The abundance and activity of the major members of the heterotrophic microbial community – from viruses to ciliates – were studied along a longitudinal transect across the Mediterranean Sea in the summer of 2008. The Mediterranean Sea is characterized by a west to-east gradient of deepening of DCM (deep chlorophyll maximum) and increasing oligotrophy reflected in gradients of biomass and production. However, within this well documented longitudinal trend, hydrological mesoscale features exist and likely influence microbial dynamics. Here we present data from a W-E transect of 17 stations during the period of summer stratification. Along the transect the production and fate of organic matter was investigated at three selected sites each one located in the centre of an anticyclonic eddy: in the Algero-Provencal Basin (St. A), the Ionian Basin (St. B), and the Levantine Basin (St. C). The 3 geographically distant eddies showed low values of the different heterotrophic compartments of the microbial food web, and except for viruses in site C, all integrated (0–150 m) stocks were higher in reference stations located in the same basin outside the eddies. During our study the 3 eddies showed equilibrium between GPP (Gross Primary Production) and DCR (Dark Community Respiration). Integrated PPp (Particulate Primary Production) values at A, B and C varied from ∼140 to ∼190 mg C m^{-2}.

Correspondence to: U. Christaki
(urania.christaki@univ-littoral.fr)

1 Introduction

The Mediterranean Sea is one of the most oligotrophic marine systems in the world. The basin-wide cyclonic circulation of nutrient-depleted water (Dugdale and Wilkerson, 1988), hot, dry climate and low land run-off contribute to the low productivity of the sea. The Mediterranean also exhibits a marked west to east gradient of oligotrophy seen in an increasing nutrient depletion from west to east (Krom et al., 1991), declines in chlorophyll concentrations (Ignatiades et al., 2009) and rates of primary production (Moutin and Raimbault, 2002; Turley et al., 2000). The hypothesis of phosphorus limitation of primary production in the Mediterranean has inspired numerous studies dealing with microbial processes in its open waters, and resulted in the

establishment of large-scale patterns of abundance and activity for different planktonic food web components (reviewed in Siokou et al., 2010). The Mediterranean is generally considered to be an oligotrophic ecosystem characterized by a microbe-dominated food web. The dominance of small heterotrophs and small phototrophs in this region is consistent with a scenario of little energy transfer to high trophic levels (cf. review by Siokou et al., 2010). Thus, microbial heterotrophic activity is an important energy pathway in the planktonic food web and in particular in the eastern Mediterranean, where most of the organic carbon produced is consumed and respired (Regaudie-de-Gioux et al., 2009). Up to 90–95 % of primary production is sustained by internal recycling of organic matter during the stratified period (Moutin and Raimbault, 2002). Turley et al., (2000) hypothesised that a large portion of primary production is directly channeled to heterotrophic prokaryotes through exudation and/or lysis of nutrient-stressed phytoplankton. Probably the most convincing evidence of P limitation of heterotrophic prokaryotes resulted from the CYCLOPS in-situ P-fertilization experiment conducted in May 2002 in the Cyprus-Eddy. In this experiment, prokaryotic heterotrophic production increased in response to P addition whereas phytoplankton biomass diminished (Thingstad et al., 2005).

Nonetheless, the Mediterranean Sea while often attributed the label "oligotrophic", shows considerable variability over a wide range of temporal and spatial scales. This variability is reflected in the microbial components of the planktonic food web. For example, in the west the Almeria-Oran front is an area of high primary production (Videau et al., 1994; Van Wambeke et al., 2004) compared to surrounding waters, while the Cyprus-Eddy in the east, is a zone of low phytoplankton production (Psarra et al., 2005).

Our study was conducted within the framework of the BOUM cruise (Biogeochemistry from Oligotrophic to the Ultra-oligotrophic Mediterranean) in the summer of 2008. The first objective was a complete description of the microbial food web, and in particular the heterotrophic components, along a W-E transect of 17 stations of the Mediterranean Sea during the period of summer water-column stratification. Our second objective was to estimate rates of the production and fate of organic matter, in 3 geographically distant oligotrophic environments located at the centre of anticyclonic eddies. The cores of persistent eddies are relatively isolated from surrounding waters, thus these sites provide possibilities for the estimation of biogeochemical fluxes. Located along the W-E transect, we expected that these three eddies would differ not only in terms of biomass and production compared to outside reference stations located in the same basin, but also among each other. The major biogeochemical and biological parameters reported in this study are microbial stocks (from viruses to ciliates) and heterotrophic prokaryotic production at all stations, while primary production and oxygen fluxes (community production and respiration) were measured only in the three eddy sites.

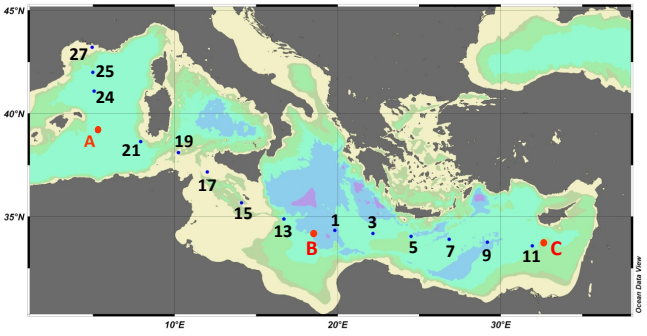

Fig. 1. Stations occupied for microbial metabolism and heterotrophic microplankton studies during the BOUM cruise (June–July, 2008). Sites A, B and C are situated in the centre of 3 anticyclonic eddies.

2 Methods

2.1 Sample collection, general characteristics of the study site

The BOUM cruise took place during the summer of 2008 (16 June–20 July, 2008). Using the French Research Vessel l'Atalante, a 3000 km transect was surveyed from the western part of the Mediterranean Sea to the Eratosthenes sea mount in the eastern part along a longitudinal transect from the Levantine basin (34° E) to the Western basin (5° E, Fig. 1). Along this transect, two types of stations were sampled: the "short duration stations" (2–3 h occupation) and "long duration sites" (4 days occupation). Except for St. 27 and 17 located on the continental slope, the stations were situated in the open sea (Fig. 1).

Biological data presented in this study are based on surface-layer sampling (8–10 depths from 0 to 200 m) of 14 representative "short duration stations" and the 3 "long duration sites" situated in the centre of anticyclonic eddies. The approximate location of the gyres were determined using satellite imagery and the forecast from MERCATOR. The exact locations of the eddies were determined on board from a rapid (12 h) high resolution survey using XBT, thermosalinograph and ADCP data to precisely locate sites with low potential advection. At each site, before starting the 96 h process study, a 24 h physical and chemical characterisation of the area was carried out. The area was surveyed by the exploration of a grid consisting of 16 sub-stations in a 9×9 miles geographic area centered around the site. Data for each sub-station were obtained from 0 to 500 m or 1000 m depth with CTD casts. The salinity and nitrate profile (Fig. 2a–c) are here presented to show the "halostad" and "nutrientstad" (large zones in depth of constant salinity or nitrate which characterize the core depth of the eddies). These "stad" correspond also to low variations with depth in density, oxygen and temperature as reported by Moutin et al. (2011). The 2 eddies B and C in the Eastern Mediterranean exhibit deep cores constituted by Levantine Intermediate water, of higher

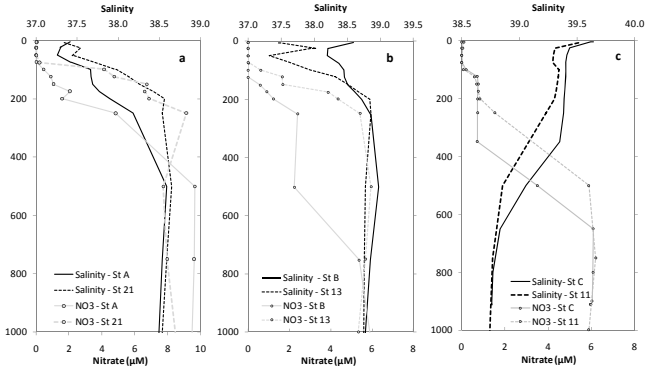

Fig. 2. Salinity and nitrate profiles inside and outside of the 3 anticyclonic eddies, dark and light solid lines – inside the eddy, respectively for salinity and nitrate, black and grey dotted lines – outside the eddy, respectively for salinity and nitrate. Nitrate values presented on this figure were discrete measurements from Niskin bottle samples.

salinity, while the core of the eddy A was formed with Surface Modified Atlantic water of lower salinity than outside the eddy (Fig. 2a). For all eddies the core density was lower and the temperature and oxygen were higher than outside the eddies at the same depths. As expected in anticyclonic eddies the eddy center at the three features was characterized by the downwelling of the isotherms and isopicnals in the upper layer.

Profiles of temperature, conductivity, oxygen and fluorescence were obtained using a Sea-Bird Electronics 911 PLUS Conductivity-Temperature Depth profiler (CTD, temperature and oxygen data are not used in this paper) and water samples using Niskin bottles with Teflon-coated springs and O-rings. Total Chlorophyll-*a* (Chl-*a* = Chlorophyll−*a* plus divinyl-Chlorophyll-*a*) was measured by High Performance Liquid Chromatography with methodology described in Ras et al. (2008). Concentrations of nitrate (NO_3) and nitrite (NO_2) and soluble reactive phosphorus, referred to the term phosphate (PO_4) in this paper, were immediately measured on board with an autoanalyser (Bran + Luebbe autoanalyser II) according to the colorimetric method (Tréguer and Le Corre, 1975). Precision of measurements was 0.02 µm, 0.005 µM and 0.005 µM for NO_3, NO_2, and PO_4 respectively, and detection limits for the procedures were 0.02 µM, 0.01 µM and 0.01 µM for NO_3, NO_2, and PO_4 respectively. Full details are given in Pujo-Pay et al. (2011).

2.2 Abundance of microbial components

Virus-like particles (VLP) and heterotrophic bacterial abundances (HBA, sensus stricto heterotrophic Bacteria + Archaea) were determined by flow cytometry. Subsamples (2 mL) were fixed with glutaraldehyde (final concentration, 0.5 %), refrigerated for 10–20 min, frozen in liquid nitrogen and stored at −80 °C (Marie et al., 1999) until analysis. Counts were made using a FACSCalibur flow cytometer (BD Sciences, San Jose, CA, USA) equipped with an air-cooled laser, providing 15 mW at 488 nm with the standard filter set-up. Virus – like particles and procaryotes were stained with SYBRGreen I, as described in detail in Marie et al. (1999) and Brussaard (2004). Populations of HBA and VLP differing in fluorescence intensity were distinguished on plots of side scatter versus green fluorescence (530 nm wave- length, fluorescence channel 1 of the instrument). FCM list modes were analysed using CellQuest Pro software (BD Biosciences, version 4.0). HBA was converted to biomass using a carbon conversion factor of 12 fg C cell^{-1} (Fukuda et al., 1998).

To enumerate heterotrophic nanoflagellates (HNF), samples (20–30 mL) were preserved using formaldehyde (final concentration of 1 %). Samples were filtered onto black Nuclepore filters (pore size, 0.8 µm) and stained with DAPI (Porter and Feig, 1980) within 5 h of sampling and stored at −20 °C until counting. HNF were enumerated using a LEITZ DMRB epifluorescence microscope at 1000x. To distinguish between autotrophic and heterotrophic nanoflagellates, autofluorescence (chlorophyll) was determined under blue light excitation.

For ciliate enumeration, samples (500 mL) were placed in opaque glass bottles and fixed with acid Lugol's solution (final concentration, 2%). The samples were stored at 4 °C in the dark until analysis (max. 3 months later). The fixed samples were allowed to settle for 3 days, then the supernatant was gently removed yielding ∼100 mL of concentrate, which was further sedimented in 100 mL Hydrobios chambers for at least 24 h. Ciliates were enumerated using a Nikon Eclipse TE2000-S inverted microscope; the whole chamber was examined at 400x. Ciliates were distinguished as aloricate, naked ciliates comprising taxa of the subclasses Choreotrichida and Oligotrichia and tintinnids of the subclass Choreotrichida, order Tintinnida (Lynn, 2008). Ciliates were grouped into 4 size groups (<20, 20–30, 30–50, >50 µm). Biovolumes of all taxa and morphotypes identified in this study were calculated using the linear dimensions of cells. Biovolumes were converted to biomass using volume-to-carbon conversion factors of 190 fg C µm^{-3} for Lugol's preserved samples (Putt and Stoecker, 1989).

2.3 Bacterial production

"Bacterial" production (BP – sensu stricto referring to heterotrophic prokaryotic production –) was estimated by the ^{3}H-leucine method at 9 depths in the 0–200 m water column. At each depth, 1.5 mL duplicate samples and a control were incubated with a mixture of L-[4,5–^{3}H] leucine (Perkin Elmer, specific activity 115 Ci mmol^{-1}) and non-radioactive leucine at final concentrations of 16 and 7 nM, respectively. Samples were incubated in the dark at in situ temperature, fixed and treated following the microcentrifugation protocol (Smith and Azam, 1992) as described in detail in Van Wambeke et al. (2011) and using a conversion factor of 1.5 kg C per mole leucine incorporated.

2.4 Primary production

Carbon fixation estimates using the ^{14}C method according to the experimental protocol detailed by Moutin and Raimbault (2002) were carried out at sites A, B and C during the first and the third day of station occupation. Samples were collected before sunrise using 12 L Niskin bottles and dispensed into 320 mL polycarbonate bottles, 3 light and one dark sample per depth, for each of 10 depths covering the euphotic zone and inoculated with 20 µCi of $NaH^{14}CO_3$ (Amersham, CFA3). To determine the quantity of added tracer, a 250 µl sample was taken at random from 3 bottles and stored with 250 µL of ethanolamine for later analysis. For time zero determinations, three samples were filtered immediately after inoculation. Then, the bottles were incubated in situ in a drifting rig for 24 h (dawn-to-dawn). The rig was equipped with a line of buoys on the surface to counterbalance and equilibrate the weight in order to maintain incubation bottles at the desired depths. Rates were measured at up to 9 depths of decreasing irradiance (75, 55, 35, 20, 10, 7, 3, 1, 0.1 %), to encompass the euphotic zone. The 0.1 % irradiance samples corresponded to 130, 160 and 147 m depth for A, B and C respectively. The incubation depths were determined before every deployment based on the irradiance depth profile measured with a PAR sensor (Photosynthetically Active Radiation). After recovery of the rig, the samples were filtered on GF/F filters under low vacuum pressure (200 mm Hg) to measure net absorption (A_N mgC m^{-3}). Filters were then flooded with 500 µL of HCl 0.5 M and stored for counting at the laboratory. In the laboratory, samples were dried over 12 h at 60 °C, the 10 mL of ULTIMAGOLD-MV scintillation fluo (Packard) were added to the filters and dpm was counted after 24 h with a Packard Tri carb 2100 TR liquid scintillation analyzer. Daily (24 h dawn-to-dawn) particulate primary production (PPp) was obtained from the difference between light and dark bottles measurements. Integrated particulate primary production PPp (mg m^{-2} d^{-1}) was calculated assuming: (1) that subsurface (about 5 m) rates are identical to surface rates (not measured); and (2) that rates are zero at 20 m below the deepest sampled depth (below the photic zone). The total integrated primary production (PP_{total}) was calculated from particulate primary production (PPp) and a percentage of extracellular release (PER), with PER defined as the percentage of dissolved primary production relative to the sum of particulate and dissolved primary production. PER during the cruise was determined from on-board incubated samples (Lopez-Sandoval et al., 2011) from selected depths of the CTD cast used for the 24 h-long in situ incubations (the first and the third day of each site occupation). We used the integrated data of particulate (PPp) and dissolved primary production (PPd) determined on their profiles to compute an averaged PER for each profile. Then we used this percentage to our own data set as follows:

$$PP_{total} = PPp/(1 - PER) \quad (1)$$

2.5 Biological oxygen fluxes

At the sites A, B and C, rates of gross primary production (GPP), dark community respiration (DCR) and net community production (NCP) were estimated from changes in the dissolved oxygen concentration over 24 h incubations carried out on the in situ rig during the first and the third day of site occupation. Rates were measured at the same depths as for PPp. For each depth, three sets of four replicate water samples were placed into 125 mL borosilicate glass bottles. The first set of samples was fixed immediately (using Winkler reagents) to measure oxygen concentrations at time 0; the second set was placed in opaque bottles and the third set in transparent bottles. The samples from the last two sets were placed on the in situ rig for incubation at the depth of sample origin, and incubated for 24 h, from dawn to dawn. Dissolved oxygen concentration was measured using an automated high-precision Winkler titration system linked to a photometric end point detector (Williams and Jenkinson, 1982). NCP was calculated as the difference in the dissolved oxygen concentration between "light" incubated samples and "time 0" samples. DCR was calculated as the difference between "dark" incubated samples and "time 0" samples. DCR rates are expressed as a negative O_2 flux. GPP is the difference between NCP and DCR (Gaarder and Gran, 1927). Results presented in this study are data integrated over 130 m (site A), 160 m (site B) and 145 m (site C). Standard errors of the rates are calculated from the standard deviation of quadruple samples sets. The mean standard error obtained was ± 0.3 mmol O_2 m^{-3} d^{-1}. The DCR was converted into CO_2 units applying a respiratory quotient of 0.8 (Lefèvre et al., 2008 and references therein).

3 Results

3.1 General and longitudinal features

The water column was characterized by the presence of the seasonal thermocline. Fluorescence profiles during the cruise indicated a distinct deep chlorophyll maximum (DCM, Table 1). The classical W-E gradient of deepening of the DCM was observed; the DCM was, in general, over 30 m deeper in the east compared to the west (Fig. 3a). Mean Chl-*a* values in the upper 150 m layer were very low, 0.1–0.2 µg L^{-1} except at the two NW stations where they were slightly higher (St. 25, 27, Table 1). Below, in order to facilitate comparison with previous studies which considered the contrast between the eastern and western Mediterranean, we will sometimes refer to E and W basins, based on the simple geographical criterion employed by Longhurst (1998). Based on this division W and E stations are considered from 27 to 19 and from 13 to C, respectively. St. 17 and 15, situated in the Straight of Sicily are not included in the comparisons E-W, but these stations are included in the overall correlations between biological variables.

Table 1. Physico-chemical and biological (range and mean) of 17 sampling stations in the upper 150 m (except St. 17 and St. 27, 0–100 m) in the Mediterranean in June–July 2008. DCM: deep Chlorophyll maximum depth, VLP: virus particles, HBA: heterotrophic bacteria, HNF: heterotrophic nanoflagellates, Cil: ciliates, BP: bacterial production, nd: no data. A, B, and C sites representing selected anticyclonic eddies are depicted in bold letters.

STATION W-E	DATE (2008)	LATI-TUDE N	LONGI-TUDE E	BOTTOM DEPTH (m)	CHL a ($\mu g\,L^{-1}$)	DCM (m)	VLP ($10^6\,mL^{-1}$)	HBA ($10^5\,mL^{-1}$)	HNF ($10^3\,mL^{-1}$)	CIL ($10\,L^{-1}$)	BP ng C L^{-1} h^{-1})
27	18/7	43.20967°	4.93050°	98	0.06–0.37 0.24	30	2.92–7.92 5.88	3.63–8.63 5.78	1.03–3.26 2.15	nd	nd
25	18/7	41.99633°	4.98550°	2267	0.004–1.7 0.32	50	1.39–12.66 5.38	0.19–1.02 0.56	1.44–4.65 2.65	5–157 45	1.3–40.7 18.2
24	18/7	41.08850°	5.05567°	2659	0.04–0.66 0.19	70	2.05–8.26 5.28	0.22–0.93 0.66	1.79–3.15 2.54	13–61 38	2.2–34.9 21.2
A	**14-16/7**	**39.10617°**	**5.30967°**	**2821**	**0.01–0.26 0.1**	**90**	**1.38–5.91 3.58**	**0.23–0.71 0.44**	**1.27–4.32 2.41**	**12–38 22**	**1.8–14.2 7.8**
21	11/7	38.63750°	7.91783°	2055	0.01–0.38 0.13	85	1.58–5.93 4.42	0.21–0.71 0.53	1.66–2.82 2.40	21–128 70	4.2–31.6 17.7
19	10/7	38.10233°	10.22550°	556	0.01–0.52 0.16	70	1.23–3.84 2.56	0.17–0.71 0.50	1.55–3.46 2.46	nd	1.7–29.6 18.9
17	9/7	37.16750°	11.99817°	116	0.06–0.26 0.13	80	2.66–4.15 3.47	0.52–0.77 0.65	1.31–3.60 2.35	27–86 58	1.7–38.9 28.5
15	8/7	35.66833°	14.10017°	580	0.04–0.3 0.13	100	0.82–3.46 2.16	0.19–0.70 0.54	1.51–2.51 2.03	nd	6.5–43.9 20.9
13	8/7	34.88500°	16.69850°	2101	0.04–0.27 0.14	93	1.00–2.80 1.99	0.35–0.68 0.53	1.07–2.19 1.52	22–58 41	5.6–35.9 19.9
B	**4–7/7**	**34.13350°**	**18.45550°**	**3008**	**0.04–0.21 0.11**	**120**	**0.38–2.97 1.53**	**0.15–0.49 0.36**	**0.79–2.35 1.35**	**17–32 22**	**2.0–17 9.2**
1	21/6	34.33050°	19.81867°	3210	0.05–0.58 0.18	85	0.7–4.34 1.34	2.17–6.65 4.57	0.65–1.73 1.20	34–90 62	2.1–20.9 10.8
3	21/6	34.18517°	22.16100°	2376	0.03–0.68 0.17	110	0.15–0.91 0.25	0.13–0.48 0.34	0.90–1.47 1.18	13–64 34	1.8–30.8 10.2
5	22/6	34.04600°	24.49,733°	2669	0.03–0.34 0.12	115	0.18–0.35 0.19	0.10–0.49 0.27	0.74–2.22 1.41	19–46 34	2.0–13.6 9.2
7	23/6	33.90317°	26.83533°	2780	0.04–0.40 0.15	100	1.27–2.45 1.79	0.22–0.54 0.40	0.88–1.73 1.27	25–71 52	2.8–18.2 11.6
9	24/6	33.76250°	29.17583°	3028	0.03–0.22 0.10	120	0.16–0.56 0.29	0.11-0.38 0.26	0.69–1.73 1.34	21–47 30	3.4–11.9 6.9
11	25/6	33.58283°	31.93000°	2495	0.03–0.24 0.09	110	0.45–1.12 0.78	0.17–0.43 0.28	0.42–1.53 1.04	17–27 21	1.5–12.6 6.4
C	**27–29/6**	**33.62650°**	**32.65283°**	**901**	**0.03–0.40 0.16**	**120**	**0.96–2.48 1.27**	**0.13–0.46 0.29**	**0.67–1.52 1.04**	**8–28 19**	**2.9–14 8.4**

Among all the parameters studied, virus-like particles (VLP) showed the highest variability as seen in the comparison of integrated abundances (Table 2). Concentrations varied from 0.15 to 12.7×10^6 VLP mL^{-1} (Table 1). Mean VLP in the upper 150 m layer was on the order of low $10^6\,mL^{-1}$ (Fig. 3b, Table 1). VLP quantities were relatable to Chl-*a* concentration (Table 3) but a tighter relationship existed between VLP and heterotrophic bacterial abundances (HBA,Table 3). The mean VLP/HBA ratio was highly variable and ranged from 3 to 96. HBA concentrations were on the order of 10^5 cells mL^{-1} (0.1 to 8.63×10^5 cells mL^{-1}, Table 1) and were clearly higher in the W than in the E basin (Fig. 3c). However, overall HBA was the parameter that showed the least variation in terms of integrated numbers along the transect (Table 2). A similar pattern was evident for bacterial production (BP) with lower volumetric values in the E and higher in the W (Fig. 3d, Table 1). Integrated values of BP ranged from 24 to 74 mg C m^{-2} d^{-1} (Table 2).

Table 2. Integrated values in the upper 150 m (except St. 17 and St. 27, 0–100 m) in the Mediterranean, in June–July 2008. VLP: virus particles, HBA: heterotrophic bacteria, HNF: heterotrophic nanoflagellates, CIL tot: total ciliates, CIL mixo: mixotrophic ciliates BP: bacterial production.

STATION W-E	VLP x10^{13} m^{-2}	HBA x10^{12} m^{-2}	HNF x10^{10} m^{-2}	CIL TOT x10^{9} m^{-2}	CIL MIXO x10^{9} m^{-2}	BP mgC m^{-2} d^{-1}
27	55	54	20	nd	nd	nd
25	66	74	37	51	15	53
24	59	68	37	54	22	64
A	**51**	**69**	**31**	**35**	**9**	**25**
21	64	76	36	96	39	57
19	34	63	33	nd	nd	53
17	35	65	26	57	21	74
15	33	82	31	nd	nd	66
13	30	75	22	58	21	67
B	**29**	**57**	**19**	**33**	**14**	**31**
1	31	63	18	84	30	34
3	7	52	18	54	32	38
5	3	45	23	55	31	34
7	27	61	19	78	40	41
9	3	39	21	45	16	26
11	12	44	15	31	12	24
C	**25**	**46**	**14**	**27**	**8**	**24**
Coeff. variation	0.6	0.2	0.3	0.4	0.5	0.4

Heterotrophic nanoflagellates (HNF, Fig. 4a) were dominated by small cells of mean equivalent spherical diameter of 2.46 µm and total abundances in the upper 150 m from a few hundreds to a few thousands cells per mL (0.42–4.65×10^3 cells mL^{-1}). A significant log-log relationship was found between HBA and HNF abundances (Table 3).

Ciliates generally showed low abundances and in particular at the far eastern stations (Table 1, Fig. 4b). Highest ciliate abundances were recorded at the DCM level or just above it. The log-log linear regression between Chl-*a* concentration (µg L^{-1}) and ciliate abundance (cell L^{-1}) in the upper 150 m was highly significant (Table 3). However this relationship was tighter in the W than in the east E (Table 3). The slopes of the regressions were not significantly different ($t_{\text{value}} = 0.41$; $df = 101$). Mixotrophs, as a portion of ciliate biomass, varied from 13 to 77 % (mean ± sd, 37 ± 14 %). An exceptionally high contribution in terms of biomass of mixotrophs (90 %) was recorded at St. 21 at the DCM level (Fig. 4c, Table 1). Planktonic ciliates were dominated by the aloricate naked forms with tintinnids being abundant only at St. 25 just below the DCM (75 m, 1164 cells L^{-1}, Fig. 4d). Log-transformed data of ciliate abundance and Chl-*a* concentration indicated a tight relationship between tintinnids and Chl-*a* followed by heterotrophic ciliates and a weaker relationship between mixotrophs and Chl-*a* (Table 3).

3.2 Comparing stocks in and outside the 3 anticyclonic eddies

Sites A, B and C were located in the centre of 3 distinct anticyclonic eddies across the trophic gradient. The physical data indicated that the 3 eddies were all at least several months old and that the process study stations were made in the centre of the eddies. The salinity and nitrate profiles, used to characterise the halostads and nutrientstads, allowed estimation of core depth of each eddy (Fig. 2a–c, Moutin et al., 2011).

The 3 eddies were generally associated with low values for different metrics of the heterotrophic compartments of the microbial food web compared to the stations located outside the eddies (Fig. 5). The differences were particularly pronounced for virus-like particles, heterotrophic bacterial abundance and HNF, and less pronounced for ciliates. Interestingly, among ciliates, mixotrophs did not show any recognizable pattern in terms of stocks from sites A to C (Fig. 5). Considering however their contribution to ciliate biomass, it was larger at sites B and C (43 % and 29 %, respectively) and lower at site A (18 %).

A key feature characterizing site A was a regular decline in phosphate and nitrate concentrations with depth contrasting with the sharp, marked nutriclines observed at the St. 21 in the Algero-Provencal Basin (Fig. 6a, b). Compared to stations outside the eddy, all the heterotrophic parameters recorded were lower and the depth profiles inside the eddy

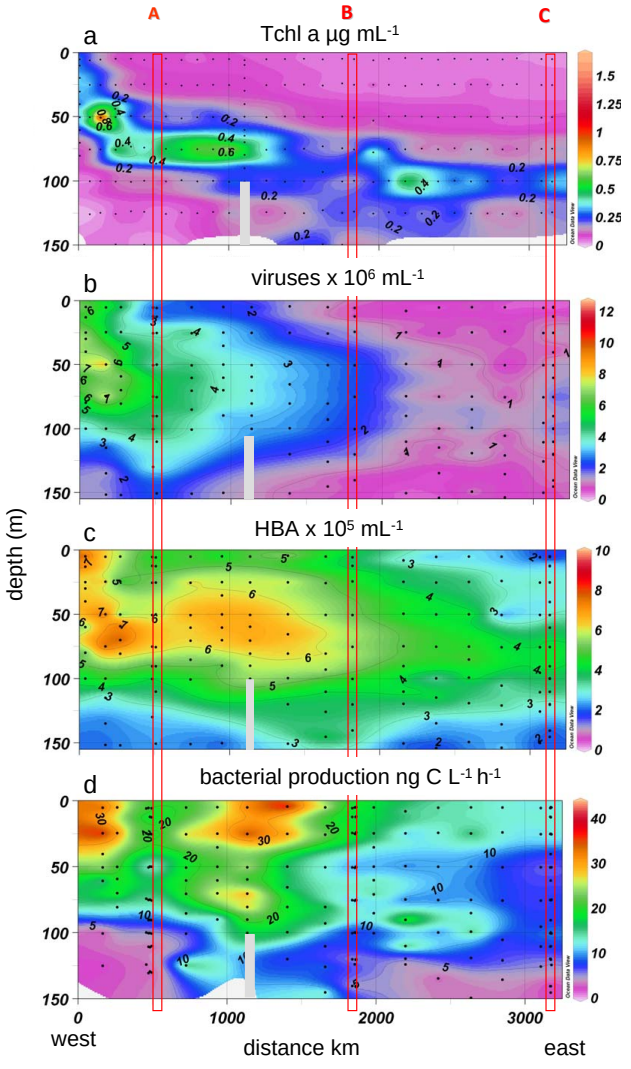

Fig. 3. Distribution of Total Chlorophyll-*a* **(a)**, virus **(b)**, heterotrophic bacteria **(c)** and bacterial production **(d)** in the upper 150 m along the Mediterranean Sea transect. Interpolation between sampling points in contour plots was made with Ocean Data View program (VG gridding algorithm, Schlitzer 2004, http://odv.awi.de/).

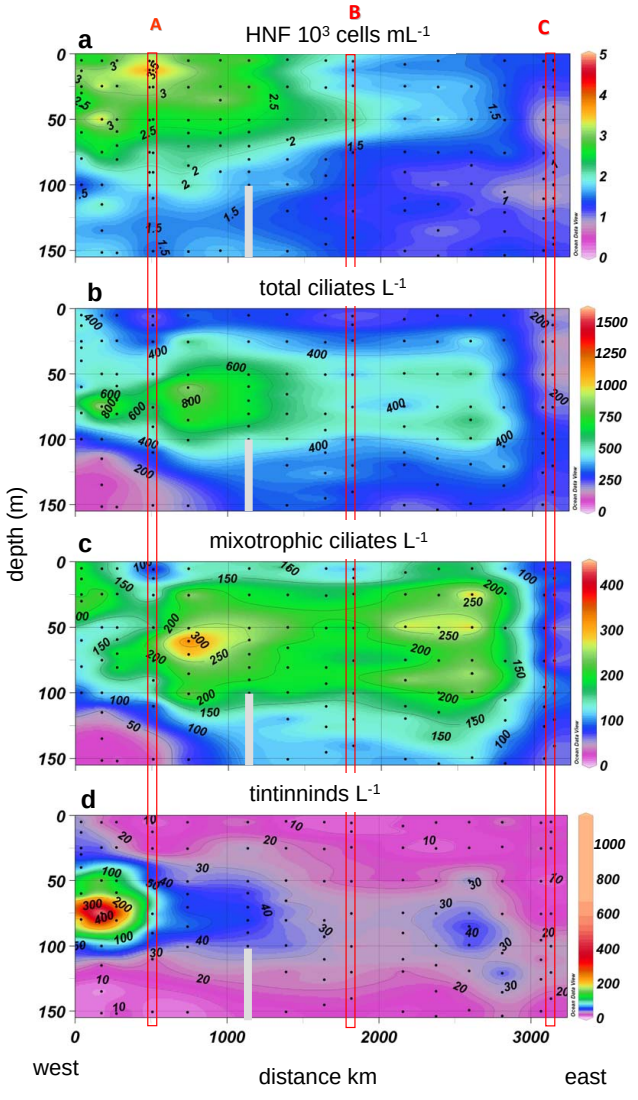

Fig. 4. Distribution of the abundance of heterotrophic nanoflagellates **(a)**, total ciliates **(b)**, mixotrophic ciliates **(c)** and tintinnids **(d)** in the upper 150 m along the Mediterranean Sea transect. Interpolation between sampling points in contour plots was made with Ocean Data View program (VG gridding algorithm, Schlitzer 2004, http://odv.awi.de/).

showed less-marked peaks (Fig. 6a–f). Mean BP was about 2 fold lower inside the eddy (Table 1) and the BP profile showed less variability with depth inside the eddy than at St. 21 where it showed several irregularities (Fig. 6a, b). The trends of HBA and VLP were very similar within and outside the eddy but concentrations were higher outside the eddy (Fig. 6c, d). HNF profiles were similar inside and outside the eddy and they did not show any particular trend with either HBA or VLP (Fig. 6c, d). Finally, the ciliate concentrations were maximal just above the DCM both within and outside the eddy but with concentrations three times higher at St. 21 (Fig. 6e, f). Interestingly, at St. 21 mixotrophic ciliates were a more important component of the ciliate community, contributing approximately 33 % of total integrated biomass, compared to 18 % of the eddy community.

The same general pattern seen at site A was found for the site B: flat nutrient profiles, with a deep nutricline, contrasting with shallower ones at St. 13 outside of the eddy (Fig. 7a, b), and generally lower values for nutrients, BP, ciliates and a less pronounced maxima for fluorescence inside the eddy (Fig. 7a–f). Notably, the fluorescence profile varied little with depth in the eddy with a weak maximum just above 150 m, while outside the eddy the fluorescence profile showed pronounced maxima. The fluorescence maxima at St. 13 were associated with the presence of *Prochlorococcus*

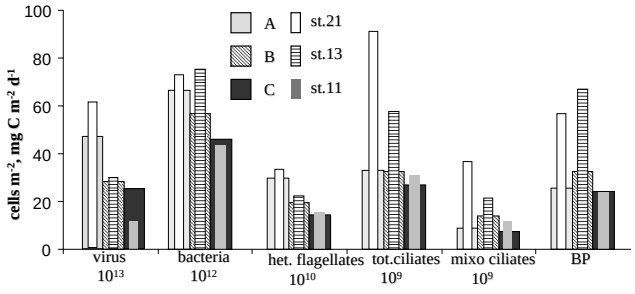

Fig. 5. Integrated values of viral particles ($10^{13}\,m^{-2}$), heterotrophic bacteria ($10^{12}\,m^{-2}$), heterotrophic nanoflagellates ($10^{10}\,m^{-2}$), total ciliates ($10^{9}\,m^{-2}$) and mixotrophic ciliates ($10^{9}\,m^{-2}$) and bacterial production (BP, mg C $m^{-2}\,d^{-1}$) in the upper 150 m, inside the eddies Sites A, B and C and outside the eddies St. 21, 13 and 11 respectively.

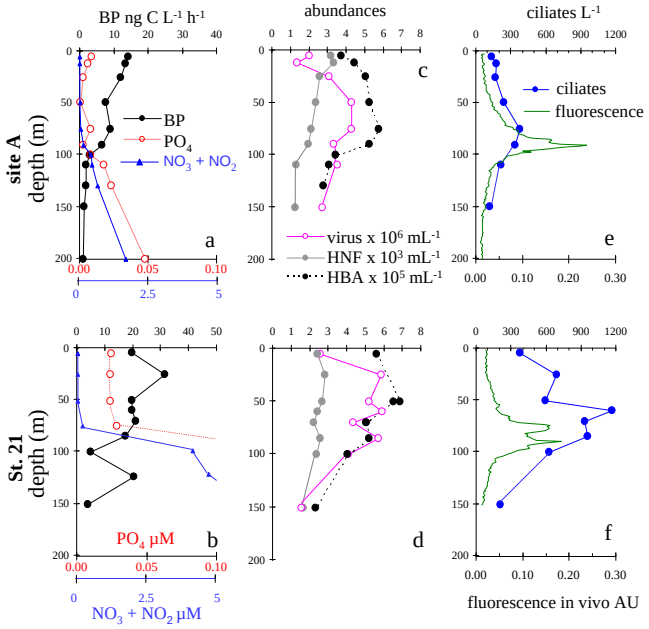

Fig. 6. Profiles of bacterial production (ng C $L^{-1}\,h^{-1}$) , PO_4 and NO_2 + NO_3 (µM) **(a, b)**, viral (VLP, $10^6\,mL^{-1}$), bacterial (HBA, $10^5\,mL^{-1}$) and heterotrophic nanoflagellate abundance (HNF, $10^3\,mL^{-1}$), **(c, d)**, ciliate abundance (L^{-1}) and in situ fluorescence **(e, f)** in the centre of the eddy A (upper panel a, c, and f) and at St. 21 (lower panel b, d and e).

at 80 m (116 10^3 cells mL^{-1}), while at 140 m the maximum of fucoxanthine was observed (0.05 µg L^{-1}) associated with the presence of *Prochlorococcus* and *Synechococcus* (1.5 and 1.5 10^3 mL^{-1}, respectively, Crombet et al., 2011). Mean bacterial production was again about 2 fold lower inside the eddy (Table 2). HBA and VLP showed similar trends in particular inside the eddy (Fig. 7c, d). HBA showed a deep maximum at the DCM outside the eddy. HNF profiles were again quite similar in terms of trend and absolute values inside and outside the eddy (Fig. 7c, d). Finally, ciliates showed in both cases maximal abundance just above the DCM and

Table 3. Determination coefficients (r^2) of some significant log-log linear regressions mentioned in the text, $p < 0.0001$ except Chl-*a*-CIL total east, where <0.001 VLP: virus particles, HBA: heterotrophic bacteria, HNF: heterotrophic nanoflagellates, CIL: ciliates, PPp: particulate primary production, BP: bacterial production, nd: no data, east: Eastern Basin, west: western basin.

Variable (x)	Variable (y)	n	r^2
Chl-*a*	VLP	116	0.13
HBA	VLP	116	0.51
HBA	HNF	153	0.29
Chl-*a*	CIL total	111	0.48
Chl-*a*	CIL total west	31	0.50
Chl-*a*	CIL total east	72	0.22
Chl-*a*	CIL tintinnids	111	0.50
Chl-*a*	CIL heterotrophs	111	0.46
Chl-*a*	CIL mixotrophs	111	0.20
PPp	BP	60	0.66
PPp site A	BP site A	20	0.81
PPp site B	BP site B	20	0.88
PPp site C	BP site C	20	0.44

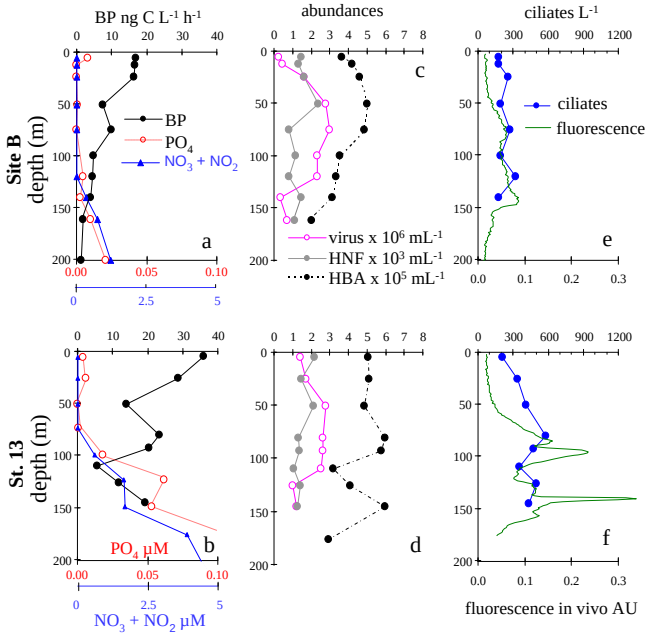

Fig. 7. Profiles of bacterial production (ng C $L^{-1}\,h^{-1}$), PO_4 and NO_2 + NO_3 (µM) **(a, b)**, viral (VLP, $10^6\,mL^{-1}$), bacterial (HBA, $10^5\,mL^{-1}$) and heterotrophic nanoflagellate abundance (HNF, $10^3\,mL^{-1}$), **(c, d)**, ciliate abundance (L^{-1}) and in situ fluorescence **(e, f)** in the centre of the eddy B (upper panel a, c, and f) and at St. 13 (lower panel b, d and e).

were about two times more abundant at St. 13 compared to inside the eddy.

Site C was situated in the ultra-oligotrophic east Mediterranean above the seamount Eratosthenes (900 m). An

Table 4. Integrated values of: Bacterial Production (BP), Particulate Primary Production (PPp ± associated standard errors, Mouriño-Carballido and McGillicuddy Jr, 2006) and Total Primary Production (PP_{total}), the first (A1, B1 and C1) and the third day (A3, B3 and C3) of site occupation. Integrated Dark Community Respiration in terms of carbon (DCR_{CO_2}) is estimated assuming respiratory quotient = 0.8, and Bacterial Carbon Demand (BCD = BP + BR) assuming that bacterial respiration was responsible for 50 % of the DCR.

	BP mg C m^{-2} d^{-1}	PPp mg C m^{-2} d^{-1}	PP_{total} mg C m^{-2} d^{-1}	DCR_{CO_2} mg C m^{-2} d^{-1}	BCD mg C m^{-2} d^{-1}	BCD/PP_{total}
A1	24.6	156 ± 5	224	525	287	1.3
A3	36.3	164 ± 2	229	554	313	1.37
B1	32.7	195 ± 4	306	430	248	0.81
B3	36.7	187 ± 5	271	452	263	0.97
C1	26.5	137 ± 3	206	373	213	1.03
C3	24.5	192 ± 8	317	546	297	0.94
A1	24.6	156 ± 5	224	525	287	1.3
A3	36.3	164 ± 2	229	554	313	1.37
B1	32.7	195 ± 4	306	430	248	0.81
B3	36.7	187 ± 5	271	452	263	0.97
C1	26.5	137 ± 3	206	373	213	1.03
C3	24.5	192 ± 8	317	546	297	0.94

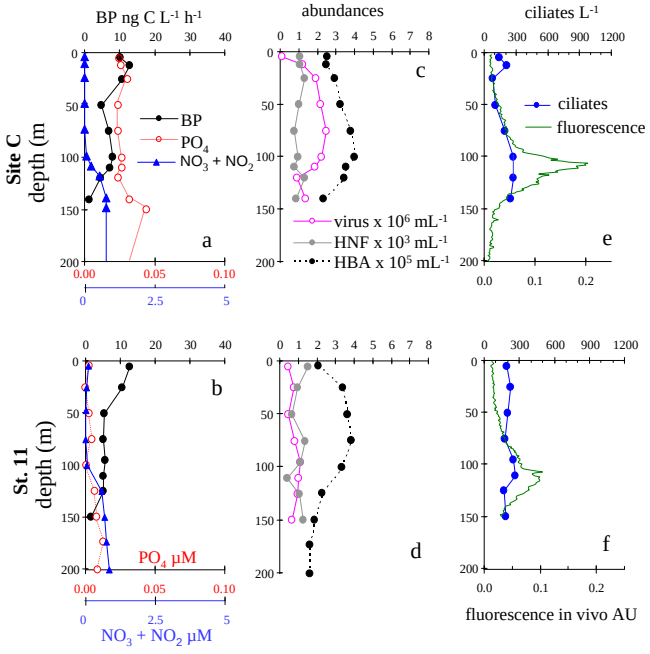

Fig. 8. Profiles of bacterial production (ng C L^{-1} h^{-1}) , PO_4 and NO_2 + NO_3 (µM) **(a, b)**, viral (VLP, 10^6 mL^{-1}), bacterial (HBA, 10^5 mL^{-1}) and heterotrophic nanoflagellate abundance (HNF, 10^3 mL^{-1}), **(c, d)**, ciliate abundance (L^{-1}) and in situ fluorescence **(e, f)** in the centre of the eddy C (upper panel a, c, and f) and at St. 11 (lower panel b, d and e).

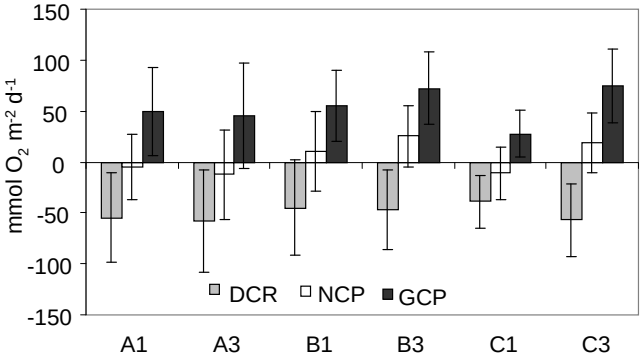

Fig. 9. Integrated GPP (Gross Primary Production), DCR (Dark Community Respiration) and NCP (Net Community Production) (mmol O_2 m^{-2} d^{-1}, 130 m site A, 160 m site B, 145 m site C), at the three eddies the first (A1, B1 and C1) and the third day (A3, B3 and C3) of site occupation. Error bars represent standard deviation of 4 replicates.

unexpected feature of this eddy was the presence of measurable phosphate in surface waters (Fig. 8a, b). Nevertheless, this result should be considered with caution because the nutrient concentration in the upper surface waters are close to the detection limits of the methods. The deep fluorescence maximum was clearly more marked in the eddy and was associated with the presence of diatoms (Crombet et al., 2011). In contrast to the eddies of sites A and sites B, the general characteristic was a similarity for all parameters – except viruses – comparing the eddy and stations outside the eddy (St. 11, Fig. 8a–f). Viruses were more abundant and showed a remarkably similar trend with HBA inside the eddy. Ciliates were found at their lowest abundances at these far-east stations with no marked differences inside and outside the eddy (Fig. 8e, f). The eddy and St. 11 ciliate communities were also similar in terms of the relative contribution of mixotrophic forms (about 29 % of total integrated biomass).

3.3 Biological fluxes in the 3 anticyclonic eddies

Particulate primary production (PPp) and oxygen fluxes were measured twice at each site (Table 4). At sites A and B the two PPp integrated values measured the 1st and the 3rd day of station occupation were similar (156 vs. 165 and 192 vs. 195 mg C m^{-2} d^{-1}, respectively), while they showed some variability at site C(136 vs. 192 mg C m^{-2} d^{-1}). Overall, values of PPp were relatable to BP and this relationship was very strong at sites A and B and weaker at C (Table 3). Integrated GPP and DCR, ranged 28–75 mmol O_2 m^{-2} d^{-1} (mean $\pm$ sd, 54 ± 18) and 39–58 mmol O_2 m^{-2} d^{-1}(mean $\pm$ sd, 50 ± 8), respectively, in the centre of the 3 eddies (Fig. 9). Similar to PPp, GPP was more variable at site C (28 and 75 mmol O_2 m^{-2} d^{-1}). Gross production roughly balanced with respiration and net community production (NCP) fluxes were not different from zero (Fig. 9). BP was measured along 4 profiles at each site (once per day). Average 0–150 m integrated values were 36.4 ± 7.6, 35.6 ± 2.9 and 27.5 ± 3.3 mg C m^{-2} d^{-1} (mean $\pm$ sd) at the sites A, B and C, respectively, and were barely statistically different only between A and C (ANOVA, $p = 0.035$)

4 Discussion

4.1 General and longitudinal features

Our first objective was a complete documentation of the vertical and longitudinal distribution of the heterotrophic components of the microbial food web through a transect of 17 stations. Previous studies have documented the W-E gradients in the Mediterranean Sea but in terms of the individual components of the microbial food web (e.g. Dolan et al., 1999; Christaki et al., 2001; Pitta et al., 2001; Van Wambeke et al., 2002). Our study is the first, to our knowledge, to have examined simultaneously all the major components of the heterotrophic microbial food web, from viruses to ciliates and furthermore estimate biological fluxes at 3 mesoscale anticyclonic eddies situated in each of the 3 Mediterranean basins. Overall, our observations concerning the longitudinal gradients were in agreement with the reported west to east trends of deepening of DCM and increasing oligotrophy in terms of biomass and production from W-E (reviewed in Siokou et al., 2010).

Among the very few previous studies of viruses in open Mediterranean waters, viral abundance reported varied between 0.8 and 16×10^6 VLP mL^{-1} (e.g. Guixa-Boixereau et al., 1999; Weinbauer et al., 2003; Magagnini et al., 2007). Our estimates of viral abundance for the early summer ranged similarly (0.16–12×10^6 VLP mL^{-1}). We found a weak relationship between Chl-*a* and VLP compared to the tight correlation of the latter with HBA (cf. results section) implying that heterotrophic bacteria are the more probable viral hosts compared to phytoplankton. Interestingly, integrated profiles of VLP and HBA showed the highest and the lowest variability, respectively (Table 2). Indeed, volumetric VLP/HBA ratio varied over a wide range (3 to 96) suggesting that viral abundance may vary over short periods of time, reflecting different phases of infection and release of host cells. HNF abundance, similar to other stocks measured in this study, was about two times higher in the west, but this parameter showed overall relatively low variability (30 %, Table 2). The significant relationship between log-log HNF and HBA values ($n = 153$, $r^2 = 0.29$, $p < 0.0001$) and the relative invariability of bacterial numbers, together, suggest that bacterial production was tightly matched by bacterial mortality.

Ciliate abundance at different stations displayed high variability with roughly a 2-fold decrease overall for ciliate standing stock from W to E, in agreement with previous studies (Dolan et al., 1999; Pitta et al., 2001; Dolan et al., 2002). Ciliates in our study showed a significant relationship with Chl-*a* and their maximum abundances were related to the DCM, similar to previous reports (Dolan and Marrasé, 1995; Dolan et al., 1999). Compiled data from different studies in the Mediterranean Sea have shown that this relationship may be stronger in the W than in the E basins (Siokou et al., 2010) as was found in our study.

The contribution of mixotrophic ciliates to total ciliate biomass was important and within the range reported in the few other existing studies of open Mediterranean waters (Pérez et al., 1997; Dolan et al., 1999; Pitta et al., 2001). In our study, we did not attempt a detailed analysis of ciliate community composition. The mixotrophic/autotrophic ciliate *Myrionecta rubra* was pooled with easily distinguished taxa of mixotrophic ciliates (*Tontonia* spp., *Laboea strobila*, *Strombidium acutum, Strombidium capitatum* and *Strombidium conicum*). The use of Lugol's fixative precluded identification of mixotrophic ciliates without distinctive gross morphology (i.e., certain small *Strombidium* species); the heterotrophic group likely contained some mixotrophs and thus our mixotroph numbers may be underestimates. However, the mixotrophs considered in our study are the larger forms which, according to Dolan et al. (1999) and Karayanni et al. (2004), likely represent most of the mixotrophic biomass. Dolan et al. (1999) and Pitta et al. (2001) reported a more important contribution of mixotrophs in the E compared to the W basin. This pattern was not clear during our study since the contribution of mixotrophs was slightly -but not significantly- lower in the W (33 ± 19 % and 39 ± 15 % in W and E, respectively). Overall, mixotrophs showed a high variability in their contribution in total ciliate biomass (Table 2) and the mixotrophs *S. acutum* and *S. capitatum* dominated ciliate biomass at St. 25 at the DCM level (Fig. 4c, 90 % of ciliate biomass). In a recent study in the western Mediterranean Sea, mixotrophs were found to be efficient grazers of nanophytoplankton forming dense populations related to high Chl-*a* concentrations (Christaki et al.,

2009). Tintinnids are also known to form patchy distributions related to their food resources (e.g., Stoecker et al., 1984; Christaki et al., 2008). Accordingly, the unique high tintinnid abundance recorded was in the W, at the station and depth where the highest concentration of Chl-*a* during BOUM cruise was measured (St. 25, Table 1, Fig. 4d).

4.2 Stocks and biological fluxes in the 3 anticyclonic eddies

A major aim of the BOUM cruise was to estimate biogeochemical fluxes in open Mediterranean waters during the period of summer water-column stratification. The biogeochemical and the stoichiometic characterisation of stations along the entire cruise transect showed the expected oligotrophic gradient from the western to the Levantine basins (Pujo-Pay et al, 2011). In our study we focussed on 3 well established anticyclonic eddies located within the west to east gradient. The centre of established anti-cyclonic eddies are known to be zones of nutrient depletion with low rates of biological activity compared to surrounding areas (e.g. Mouriño-Carballido 2009). However, a large variety of relative activity rates have been reported with regard to cyclonic compared to anti-cyclonic eddies as well as eddies of different ages (Mouriño-Carballido and McGillicuddy, 2006). These authors during a study in the oligotrophic Sargasso Sea have reported that positive rates occurred in younger cyclones and in areas of eddy-eddy interactions, whereas negative NCP rates were observed in anticyclones and older cyclone features that were decaying. Baltar et al. (2010) reported unusual results as both cyclonic and anticyclonic (both "young & mature") eddies were described as showing high prokaryote activities both per cell and as bulk rates, interestingly with no differences in community composition in surface layer communities. Most commonly, increases in heterotrophic activity characterize cyclonic eddies, immature "cold core" eddies. More importantly however, very few studies have attempted to estimate overall metabolism through comparing phytoplankton production, bacterial production and community respiration. Thus, our goal was not simply to compare prokaryotes inside and outside the eddies but rather to gauge their activity relative to the other components of the planktonic food web. The three sites investigated were located along a longitudinal axis corresponding with a gradient of increasing oligotrophy and were expected to differ, at least according to their location along the well-described east-west gradient of increasing oligotrophy in the Mediterranean.We found that the 3 eddies were indeed associated with low values for different metrics of the heterotrophic compartments of the microbial food web compared to the stations located outside the eddies. Metazooplankton biomass was also found to be lower inside the eddies compared to stations outside the eddies (Nowaczyk et al., 2011).

While the W-E gradient among the eddies was generally recognizable in terms of heterotrophic biomass (Fig. 5), the same was not true for fluxes. Integrated PPp (Particulate Primary Production) values at A, B and C varied from ∼140 to ∼190 mg C m^{-2}. Surface oxygen production roughly balanced by respiration. NCP was not significantly different from zero in all three sites (4 ± 15 mmol O_2 m^{-2} d^{-1}) (Fig. 9) showing systems in metabolic balance (Williams, 1993).

Athough, we have no explanation for the variability found between the two station C experiments, the relatively high PPp at site C was rather unexpected in the sense that it diverged from the established W-E decreasing productivity gradient as it was equal to, or even higher than (on the second day), values with sites B and A. Moreover, compared to previous estimates (May 2002) in the warm core Cyprus-eddy during the CYCLOPS experiment (Psarra et al., 2005), Chl-*a* and PPp values reported here are 2-fold higher. If we compare site C to the western site A, there are several interesting differences. The elevated integrated PPp values at station C may be attributed to a deep maximum recorded at 80–100 m depth, since values in the 0–80 m layer were lower than those at sites A and B (data not shown). Interestingly, these deep PPp and Chl-*a* maxima are mostly associated with an N/P < 10 and the presence of diatoms and prymnesiophytes whereas the respective maxima of Chl-*a* at site A (90 m) are associated with an N/P > 25 and the presence of cyanobacteria and prymnesiophytes (Crombet et al., 2011). Interpretation of this peculiar character of site C is not straightforward. A plausible explanation might be the presence of detectable, phosphate concentration (30 nM) in the entire surface layer (0–150 m), whereas they were below detection limits in the surface layers of sites A and B, despite a deeper phosphacline at site C. The origin of the higher PO_4 concentrations at site C remains obscure. Probably, the elevated phytoplankton biomass and production observed at site C were related to the higher PO_4 concentrations, at an optimum depth (80–100 m) where there was enough nitrate and nitrite and light to sustain productivity and growth. Most probably, the bottom topography and vertical structure of the eddy at site C (warmer and shallower) may have played a critical role in structuring nutrient profiles (for full details on the physics, Moutin et al., 2011). Based on these observations, we might argue that mesoscale activity alone is not always sufficient to interpret the microbial food web dynamics within the Mediterranean eddies, and the complexities engendered by particular geographic or seasonal characteristics, hydrodynamics and external inputs require consideration.

With the exception of a seasonal study at a fixed station in the Ligurian Sea (Lemée et al., 2002) and a late-spring early summer cruise in the open Mediterranean Sea by Regaudie-de Gioux et al. (2009), very few data on planktonic O_2 metabolism exists for the Mediterranean Sea and they are mostly restricted to coastal/frontal areas of the

Western Mediterranean (Lefèvre et al., 1997; Navaro et al., 2004; Van Wambeke et al., 2004). Our integrated GPP (28–75 mmol O_2 m^{-2} d^{-1}) and DCR (39–58 mmol O_2 m^{-2} d^{-1}) values fall within the range of previously recorded values except the ones reported by Regaudie-de Gioux et al., (2009), which were higher (mean GPP 118–196 mmol O_2 m^{-2} d^{-1}).

The mean integrated value in the eddies matches the mean integrated BP of the deep, open sea stations of the E basin (39 ± 15 mg C m^{-2} d^{-1}) and was clearly lower than the mean integrated BP of the deep, open sea stations of the W basin (61 ± 7 mg C m^{-2} d^{-1}, Van Wambeke et al., 2011), corresponding to the oligotrophic nature of the eddies. The integrated bacterial production values obtained in the 2 basins were similar to those ones previously reported for open Mediterranean Sea waters (e.g. Pedros-Alio et al., 1999; Christaki et al., 2001; Van Wambeke et al., 2002, 2004).

The mean PPp values obtained in the three eddies are situated at the lower range of values reported previously in open Mediterranean Sea waters (e.g. Moutin and Raimbault, 2002) using the same JGOFS protocol. The integrated BP/PPp ration was on average 0.17 ± 0.04 over the 3 sites and corresponded to the ratio generally found in oligotrophic environments (Ducklow, 2000). It is probable that the coupling of the two production processes is high as shown by the strong positive relationship between volumetric BP and PPp data (e.g., Turley et al., 2000).

However, PPp is not all of the net primary production, and estimates of PPd are needed to accurately compare primary production with bacterial carbon demand. Unfortunately, little information is available on percentages of extracellular release of photosynthate in the Mediterranean Sea, data which is needed to compute total primary production, PP_{total} (excluding heterotrophic respiration and photorespiration). During the BOUM cruise, the percentage of PER was determined 3 times in each eddy (Lopez-Sandoval et al., 2011). PER was significantly lower at site A compared to C (ANOVA test, $p = 0.01$), with means of 29 ± 1, 35 ± 3 and 39 ± 5 at sites A, B and C, respectively. The largest variability of PER, from one day to another at one given eddy, was found for the site C. This relatively high variability was also seen for PPp and GPP, and for this reason for computing PP_{total} we used each profile's values instead of means (Table 4).

Bacterial respiration (BR) was not measured during our study. Some data from previous reports exists on the contribution of bacterial respiration (BR) to Dark Community Respiration (DCR) in the Mediterranean Sea. In the NW Mediterranean Sea, at the open water DYFAMED site, the mean ratio BR/DCR over an annual cycle in the euphotic zone was 67 % (Lemée et al., 2002). In another annual cycle study in oligotrophic coastal Mediterranean Sea waters, an average value of 52 % (range 25 to 97 %) was recorded by Navarro et al. (2004). BR ranged from undetectable to 3.18 mmol O_2 L^{-1} d^{-1} (Lemée et al., 2002) and from 0.27 to 3.64 mmol O_2 L^{-1} d^{-1} (Navarro et al., 2004). BR was not measured during BOUM cruise. However, assuming that BR accounted for 50 % of DCR, then the Bacterial Growth Efficiency (BGE = BP/(BP + BR)) would be on average 11 ± 2 % in the 3 eddies (based on integrated data of Table 4). Generally BGE tends to be low in oligotrophic systems, perhaps because most of the DOC pool is recalcitrant and inorganic nutrients are scarce (del Giorgio et al., 1997). Indeed, in the Almeria-Oran geostrophic front and adjacent Mediterranean waters BGE was estimated to be 7 % (Sempéré et al., 2003) and lower values (2.6 ± 0.1 %) were obtained in the NW-Mediterranean through a coastal offshore gradient (Moran et al., 2002). Therefore, a BGE estimate of 11 % which may be high, argues that BR represented at least 50 % of DCR. Based on these assumption, PP_{total} was sufficient to sustain bacterial carbon demand at sites B and C where fluxes were not significantly different (Table 4) while this was not the case at site A. At this site, ratio BCD/PP_{total} ranged 1.3–1.4 and was in accordance with NCP (although not statistically different from zero, values were slightly higher than 1). Such comparisons highlight that estimates of dissolved primary production are necessary to compare metabolic balances derived from carbon fluxes versus oxygen fluxes.

Indeed, NCP varies with geographical, temporal, seasonal scales and is also strongly influenced by mesoscale variability (del Giorgio and Duarte 2002; Maixandeau et al., 2005). It has been shown also to vary rapidly in two E-W Mediterranean transects (Regaudie-de Gioux et al., 2009).

Our study showed that within a gradient of oligotrophy, mesoscale features can be associated with zones of distinct trophic status. Furthermore, over short time periods, metabolic budgets can change rapidly (e.g. as found at site C). Temporal variability over short time-periods of a few days suggests that characterisation of metabolic balance (i.e., diagnoses of net autrophy or heterotrophy) should not be made from single measurements in space and time, particularly in oligotrophic environments where low oxygen fluxes are difficult to estimate with accuracy. Overall our results document spatial variability in microbial processes and community composition, as well as temporal variability of metabolic rates. While predicting such variability remains a challenge, consideration of both spatial and temporal heterogeneity likely requires incorporation into models of system budgets and basin functioning.

Acknowledgements. This is a contribution of the BOUM (Biogeochemistry from the Oligotrophic to the Ultraoligotrophic Mediterranean) experiment (http://www.com.univ-mrs.fr/BOUM) of the French national LEFE-CYBER program, the European IP SESAME and the international IMBER project. The BOUM experiment was coordinated by the Institut des Sciences de l'Univers (INSU) and managed by the Centre National de la Recherche Scientifique (CNRS).We also thank Josephine Ras for pigment analysis. We thank the reviewers for their comments and http://www.anglais.webs.com/ for english corrections.

Edited by: C. Jeanthon

The publication of this article is financed by CNRS-INSU.

References

Baltar, F., Aristegui, J., Gasol, J. M., and Lekunberri, I.: Mesoscale eddies: hotspots of prokaryotic activity and differential community structure in the ocean, ISME J., 4, 975–988, 2010.

Brussaard, C. P. D.: Optimization of procedures for counting viruses by flow cytometry, Appl. Environ. Microbiol., 70, 1506–1513, 2004.

Christaki, U., Giannakourou, A., Van Wambeke, F., and Gregori, G.: Nanoflagellate predation on auto- and heterotrophic picoplankton in the oligotrophic Mediterranean Sea, J. Plankton Res., 23, 1297–1310, 2001.

Christaki, U., Obernosterer, I., Van Wambeke, F., Veldhuis, M., Garcia, N., and Catala, P.: Microbial food web structure in a naturally iron fertilized area in the Southern Ocean (Kerguelen Plateau), Deep Sea Res. Pt. II., 55, 706–719, 2008

Christaki, U., Courties, C. Joux, F., Jeffrey, W. H., Neveux, J., and Naudin, J. J.: Community structure and trophic role of ciliates and heterotrophic nanoflagellates in Rhone River diluted mesoscale structures (NW Mediterranean Sea), Aquat. Microb Ecol., 57, 263–277, 2009.

Crombet, Y., Leblanc, K., Quéguiner, B., Moutin, T., Rimmelin, P., Ras, J., Claustre, H., Leblond, N., Oriol, L., and Pujo-Pay, M.: Deep silicon maxima in the stratified oligotrophic Mediterranean Sea, Biogeosciences, 8, 459–475, doi:10.5194/bg-8-459-2011, 2011.

del Giorgio, P., Cole, J., and Cimbleris, A.: Respiration rates in bacteria exceed phytoplankton production in unproductive aquatic systems, Nature, 385, 148–151, 1997.

Del Giorgio, P. A. and Duarte, C. M.: Respiration in the open ocean, Nature, 420, 379–384, 2002.

Dolan, J. R. and Marrasé, C.: Planktonic ciliate distribution relative to a deep chlorophyll maximum: Catalan Sea, N. W. Mediterranean, Deep-Sea Res. Pt. I, 42, 1965–1987, 1995.

Dolan, J. R., Claustre, H., Carlotti, F., Plouvenez, S., and Moutin, T.: Microzooplankton diversity: relationships of tintinnid ciliates with resources, competitors and predators from the Atlantic Coast of Morocco to the Eastern Mediterranean, Deep-Sea Res. Pt. I, 49, 1217–1232, 2002.

Dolan, J., Vidussi, F., and Claustre, H.: Planktonic ciliates in the Mediterranean Sea: longitudinal trends, Deep-Sea Res. Pt. I, 46, 2025–2039, 1999.

Ducklow H.: Bacterial Production and Biomass in the ocean. In Microbial Ecology of the Oceans. Edited by David L. Kirchman, Wiley-Liss, Inc Nexw-York, 85–120, 2000.

Dugdale, R. C. and Wilkerson, F. P.: Nutrient sources and primary production in the eastern Mediterranean, Oceanol. Acta, Special Issue, 179–184, 1988.

Fukuda, R., Ogawa, H., Nagata, T., and Koike, I.: Direct determination of carbon and nitrogen contents of natural bacterial assemblages in marine environments, Appl. Envir. Microbiol., 64, 3352–3358, 1998.

Gaarder, T. and Gran, H. H.: Investigation of the production of plankton in the Oslo Fjord, Rapp. P.-v. Cons. int. Explor. Mer, 42, 1–48, 1927.

Guixa-Boixereu, N., Vaqué , D., Gasol, J., and Pedros-Alio, C.: Distribution of viruses and their potential effect on bacterioplankton in an oligotrophic marine system, Aquat. Microb. Ecol., 19, 205–213, 1999.

Ignatiades, L., Gotsis-Skretas, O., Pagou, K., and Krasakopoulou, E.: Diversification of phytoplankton community structure and related parameters along a large-scale longitudinal eastwest transect of the Mediterranean Sea, J. Plankton Res., 31, 411–428, 2009.

Karayanni, H., Christaki, U., Van Wambeke, F., and Dalby A.: Evaluation of double formol – lugol fixation in assessing number and biomass of oligotrich heterotrophs, mixotrophs and tintinnids. An example of estimations at mesoscale in NE Atlantic, J Microbiol. Methods, 54, 349-358, 2004.

Krom, M. D., Kress, N., Brenner, S., and Gordon, L.: Phosphorous limitation of primary productivity in the Eastern Mediterranean Sea, Limnol. Oceanogr., 36, 424–432, 1991.

Lefèvre, D., Minas, H. J., Minas, M., Robinson, C., Williams, P. J. Le B, and Woodward, E. M. S.: Review of gross community production, primary production, net community production and dark community respiration in the Gulf of Lions, Deep-Sea Res. Pt. II, 44, 801–832, 1997.

Lefèvre, D., Guigue, C., and Obernosterer, I.: The metabolic balance at two contrasting sites in the Southern Ocean: The iron-fertilized Kerguelen area and HNLC waters, Deep-Sea Res. Pt. II, 55, 766–776, 2008.

Lemée, R., Rochelle-Newall, E., Van Wambeke, F., Pizay, M., Rinaldi, P., and Gattuso, J.: Seasonal variation of bacterial production, respiration and growth efficiency in the open NW Mediterranean Sea, Aquat. Microb. Ecol., 29, 227–237, 2002.

López-Sandoval, D. C., Fernàndez, A., and Marañón, E.: Dissolved and particulate primary production along a longitudinal gradient in the Mediterranean Sea, Biogeosciences, 8, 815–825, doi:10.5194/bg-8-815-2011, 2011.

Lunghurst, A.: Ecological geography of the sea. Academic Press, San Diego, 398 p., ISBN O-12-455558-6, 1998.

Lynn, D. H.: The ciliated protozoa: characterization, classification,and guide to the literature, 3 Edn., Berlin, Springer, 606 pp, 2008.

Magagnini, M., Corinaldesi, C., Monticelli, L. S., De Domenico, E., and Danovaro, R.: Viral abundance and distribution in mesopelagic and bathypelagic waters of the Mediterranean bacteria in an oligotrophic sea-the Mediterranean and biogeochemical implications, Mar. Ecol.-Prog. Ser., 193, 11–18, 2000.

Maixandeau, A., Lefèvre, D., Karayanni, H., Christaki, U., Van Wambeke, F., Thyssen, M., Denis, M., Fernadez, C., Uitz, J., Leblanc, K., and Quéguiner, B .: Respiration in relation to microbial food web structure in Northeastern Atlantic Ocean, J. Geophys. Res., 10, C07S17, doi:1029/2004JC002694, 2005.

Marie, D., Brussaard, C. P. D., Partensky, F., and Vaulot, D.: Flow cytometric analysis of phytoplankton, bacteria and viruses. Current Protocols in Cytometry, John Wiley & Sons, Inc., 11.11.1-

11.11.15, 1999.
Moran, X. A. G., Estrada, M., Gasol, J. M., and Pedros-Alio, C.: Dissolved primary production and the strength of phytoplankton–bacterioplankton coupling in contrasting marine regions, Microb. Ecol., 44, 217–223, 2002.
Mouriño-Carballido, B. and McGillicuddy Jr, D. J.: Mesoscale activity in the metabolic balance of the Sargasso Sea, Limnol. Oceanogr., 51, 2675–2689, 2006.
Mouriño-Carballido, B.: Eddy-driven pulses of respiration in the Sargasso Sea. Deep-Sea Res. Pt. I, 56, 1242–1250, 2009.
Moutin, T., Raimbault, P., and Poggiale, J.-C.: Primary production in surface waters of the western Mediterranean sea. Calculation of daily production, Comptes Rendus de l'Academie des Sciences – Series III – Sciences de la Vie, 322, 651–659, 1999.
Moutin, T. and Raimbault, P.: Primary production, carbon export and nutrients availability in western and eastern Mediterranean Sea in early summer 1996 (MINOS cruise), J. Mar. Syst., 33, 273–288, 2002.
Moutin, T., Van Wambeke, F., and Prieur, L.: Introduction to the Biogeochemistry from the Oligotrophic to the Ultraoligotrophic Mediterranean experiment: the BOUM program, in prep., 2011.
Navarro, N., Agusti, S., and Duarte, C. M.: Plankton metabolism and dissolved organic carbon use in the Bay of Palma, NW Mediterranean Sea, Aquat. Microb. Ecol., 37, 47–54, 2004.
Nowaczyk, A., Carlotti, F., Thibault-Botha, D., and Pagano, M.: Metazooplankton diversity, community structure and spatial distribution across the Mediterranean Sea in summer: evidence of ecoregions, Biogeosciences Discuss., 8, 3081–3119, doi:10.5194/bgd-8-3081-2011, 2011.
Pedros-Alio, C., Calderon-Paz, J., Guixa-Boixereu, N., Estrada, M., and Gasol, J.: Bacterioplankton and phytoplankton biomass and production during summer stratification in the northwestern Mediterranean Sea, Deep-Sea Res. Pt. I, 46, 985–1019, 1999.
Peréz, M., Dolan, J., and Fukai, E.: Planktonic oligotrich ciliates in the NW Mediterranean: growth rates and consumption by copepods, Mar. Ecol.-Prog. Ser., 155, 89–101, 1997.
Pitta, P., Giannakourou, A., and Christaki, U.: Planktonic ciliates in the oligotrophic Mediterranean Sea: longitudinal trends of standing stocks, distributions and analysis of food vacuole contents, Aquat. Microb. Ecol., 24, 297–311, 2001.
Psarra, S., Zohary, T., Krom, M. D., Mantoura, R. F. C., Polychronaki, T., Stambler, N., Tanaka, T., Tselepides, A., and Thingstad, F. T.: Phytoplankton response to a Lagrangian phosphate addition in the Levantine Sea (Eastern Mediterranean), Deep-Sea Res. Pt. II, 52, 2944–2960, 2005.
Porter, K. G. and Feig, Y. S.: The use of DAPI for identifying and counting aquatic microflora, Limnol. Oceanogr., 25, 943–948, 1989.
Pujo-Pay, M., Conan, P., Oriol, L., Cornet-Barthaux, V., Falco, C., Ghiglione, J.-F., Goyet, C., Moutin, T., and Prieur, L.: Integrated survey of elemental stoichiometry (C, N, P) from the western to eastern Mediterranean Sea, Biogeosciences, 8, 883–899, doi:10.5194/bg-8-883-2011, 2011.
Putt, M. and Stoecker, D.K.: An experimentally determined carbon : volume ratio for marine "oligotrichous" ciliates from estuarine and coastal waters. Limnol. Oceanogr., 34, 1097–1103, 1989.
Ras, J., Claustre, H., and Uitz, J.: Spatial variability of phytoplankton pigment distributions in the Subtropical South Pacific Ocean: comparison between in situ and predicted data, Biogeosciences, 5, 353–369, doi:10.5194/bg-5-353-2008, 2008.
Regaudie-de-Gioux, A., Vaquer-Sunyer, R., and Duarte, C. M.: Patterns in planktonic metabolism in the Mediterranean Sea, Biogeosciences, 6, 3081–3089, doi:10.5194/bg-6-3081-2009, 2009.
Schlitzer, R.: Ocean Data View, http://odv.awi.de, 2004.
Sempéré, R., Dafner, E., Van Wambeke, F., Lefèvre, D., Magen, C., Allère, S., Bruyant, F., Almeria-Oran Front in the Mediterranean Sea: Implications for carbon cycling in the western basin, J. Geophys. Res., 108, 3361, doi:10.1029/2002JC001475, 2003.
Siokou-Frangou, I., Christaki, U., Mazzocchi, M. G., Montresor, M., Ribera d'Alcalá, M., Vaqué, D., and Zingone, A.: Plankton in the open Mediterranean Sea: a review, Biogeosciences, 7, 1543–1586, doi:10.5194/bg-7-1543-2010, 2010.
Smith, D. C. and Azam, F.: A simple, economical method for measuring bacterial protein synthesis rates in sea water using 3H-Leucine, Mar. Microb. Food Webs, 6, 107–114, 1992.
Stoecker, D. K., Davis, L. H., Andersen, D. M.: Fine scale spatial correlations between planktonic ciliates and dinoflagellates, J. Plank. Res., 6, 829–842, 1984.
Thingstad, F. T., Krom, M. D., Mantoura, R., Flaten, G., Groom, S., Herut, B., Kress, N., Law, C., Pasternak, A., Pitta, P., Psarra, S., Rassoulzadegan, F., Tanaka, T., Tselepides, A., Wassmann, P., Woodward, E., Wexels, Riser, C., Zodiatis, G., and Zohary, T.: Nature of phosphorus limitation in the ultraoligotrophic Eastern Mediterranean, Science, 309, 1068–1071, 2005.
Turley, C., Bianchi, M., Christaki, U., Conan, P., Harris, J. R. W., Psarra, S., Ruddy, G., Stutt, E., Tselepides, A., and Van, Wambeke, F.: Relationship between primary producers and bacteria in an oligotrophic sea-the Mediterranean and biogeochemical implications, Mar. Ecol.-Prog. Ser., 193, 11–18, 2000.
Tréguer, P. and Le Corre, P.: Manuel d'analyses des sels nutritifs dans l'eau de mer, Laboratoire d'Océanographie Chimique. Université de Bretagne Occidentale, Brest, 110 pp., 1975.
Van Wambeke, F., Christaki, U., Giannakourou, A., Moutin, T., and Souvemerzoglou, K.: Longitudinal and vertical trends of bacterial limitation by phosphorus and carbon in the Mediterranean Sea, Microb. Ecol., 43, 119–133, 2002.
Van Wambeke, F., Lefèvre, D., Prieur, L., Sempéré, R., Bianchi, M., Oubelkheir, K., and Bruyant, F.: Distribution of microbial biomass, production, respiration, dissolved organic carbonand factors controlling bacterial production across a geostrophic front (Almeria-Oran, SW Mediterranean Sea), Mar. Ecol.-Prog. Ser., 269, 1–15, 2004.
Van Wambeke, F., Catala, P., and Lebaron, P.: Vertical and longitudinal gradients in HNA-LNA abundances and cytometric characteristics in Mediterranean Sea, Biogeosciences, in press, 2011.
Videau, C., Sournia, A., Prieur, L., Fiala, M.: Phytoplankton and primary production characteristics at selected sites in the geostrophic Almeria-Oran front system (SW Mediterranean Sea), J. Mar. Syst., 5, 235–250, 1994.
Weinbauer, M., Brettar, I., and Höfle, M.: Lysogeny and virus induced mortality of bacterioplankton in surface, deep, and anoxic marine waters, Limnol. Oceanogr., 48, 1457–1465, 2003.
Williams, P. J. L. and Jenkinson, N. W.: A transportable microprocessor-controlled precise Winkler titration suitable for field station and shipboard use, Limnol. Oceanogr., 27, 576–584, 1982.
Williams, P. J. le B.: Chemical and tracer methods of measuring plankton production, ICES Mar. Sci. Symp., 197, 20–36, 1993.